ACS APPLIED MATERIALS & INTERFACES

Research Article

www.acsami.org

Assembly of Polyelectrolyte Multilayer Films on Supported Lipid Bilayers To Induce Neural Stem/Progenitor Cell Differentiation into Functional Neurons

I-Chi Lee*,† and Yu-Chieh Wu†

†Graduate Institute of Biochemical and Biomedical Engineering, Chang-Gung University, No. 259, Wenhua First Road, Guishan Township, Taoyuan County, 33302, Taiwan (R.O.C.)

Supporting Information

ABSTRACT: The key factors affecting the success of neural engineering using neural stem/progenitor cells (NSPCs) are the neuron quantity, the guidance of neurite outgrowth, and the induction of neurons to form functional synapses at synaptic junctions. Herein, a biomimetic material comprising a supported lipid bilayer (SLB) with adsorbed sequential polyelectrolyte multilayer (PEM) films was fabricated to induce NSPCs to form functional neurons without the need for serum and growth factors in a short-term culture. SLBs are suitable artificial substrates for neural engineering due to their structural similarity to synaptic membranes. In addition, PEM film adsorption provides protection for the SLB as well as the ability to vary the surface properties to evaluate the effects of physical and mechanical signals on NSPC differentiation. Our results revealed that NSPCs were inducible on SLB−PEM films consisting of up to eight alternating layers. In addition, the process outgrowth length, the percentage of differentiated neurons, and the synaptic function were regulated by the number of layers and the surface charge of the outermost layer. The average process outgrowth length was greater than 500 μm on SLB-PLL/PLGA (n = 7.5) after only 3 days of culture. Moreover, the quantity and quality of the differentiated neurons were obviously enhanced on the SLB−PEM system compared with those on the PEM-only substrates. These results suggest that the PEM films can induce NSPC adhesion and differentiation and that an SLB base may enhance neuron differentiation and trigger the formation of functional synapses.

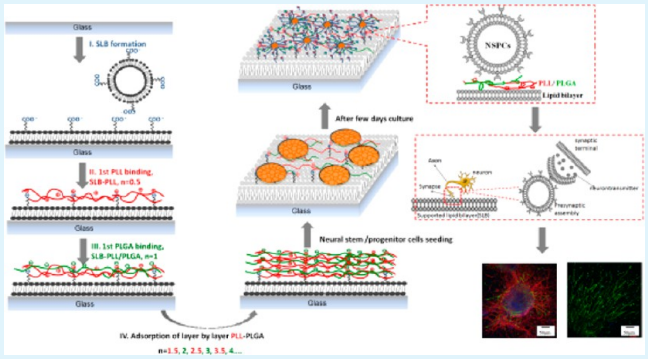

KEYWORDS: *supported lipid bilayer (SLB), synapse-triggering base, polyelectrolyte multilayer (PEM) films, neural stem/progenitor cells (NSPCs), functional neuron*

1. INTRODUCTION

The guidance of neurite outgrowth, the regulation of stem cell niches, and the induction of functional neurons are the critical components in neural regenerative medicine and neural engineering.[1−7] On the basis of these requirements, a supported lipid bilayer (SLB) was introduced in this study as a biomimetic platform for studying the behavior of neural stem/progenitor cells (NSPCs) and as a new approach for the design of functional susbtrates that can induce the formation of neurons.

Recently, stem cell engineering has focused on the development of model systems that can direct stem cell fate by providing biomaterials that mimic the native microenvironment and allow organized tissue regeneration.[2,4,5] However, the induction of NSPCs may not be optimized due to the poor viability and functionality of the induced cells[4] as well as the difficulty of inducing NSPCs to differentiate into nonglial cell types.[8−10] Therefore, inducing NSPC differentiation into specific neural types and ensuring neuron functionality are important research directions. However, the complexity of stem cell niches is challenging to reproduce. The in vitro differentiation of NSPCs into neurons has been examined using a variety of methods to control the extrinsic microenvironmental variation and to regulate the protein expression; these methods include supplementation with growth factors, cytokines, biophysical stimuli, and variations in surface properties.[11−17] Nevertheless, the substrate effects on the NSPC niche have rarely been discussed.

It has been shown that a synthetic SLB is a nonfouling surface that resists protein adsorption and prevents nonspecific molecular and cellular interactions. Among synthetic materials, SLBs demonstrate a fluidity that most closely mimics the live cell surface and retains the functional aspects of natural protein behavior in vitro.[18−22] SLBs that incorporate biospecific ligands or are functionalized with adsorbed biomacromolecules could provide a valuable system for studying cell−macromolecule

Received: June 12, 2014
Accepted: August 11, 2014
Published: August 11, 2014

interactions and cell−cell interactions.[18,21] SLBs are also considered to be suitable candidates for neural systems due to their structural similarity to synaptic membranes, the asymmetric sites of cell−cell contact between neurons and their targets.[23−26] Lucido et al. revealed that poly-D-lysine (PDL)-coated beads could induce the formation of functional presynaptic boutons.[25] Therefore, SLBs could provide new insights regarding the role of the physical and mechanical properties of cell membranes in triggering synapses and have the potential to induce the differentiation of NSPCs into functional neurons. In addition, it is well-known that astrocytes are one of the main components of the central nervous system and are tightly connected to neurons during embryonic development and adulthood.[27] It is possible that an SLB with a biomimetic and fluidic structure may also provide support similar to that provided by astrocytes.

Layer-by-layer assembled polyelectrolyte multilayer (PEM) films have been widely studied in the past decade, and they offer a simple and versatile tool for controlling surface properties.[28−33] Among the materials that have been used to make PEM films, native polypeptides, poly-L-lysine (PLL), poly-L-glutamic acid (PLGA), hyaluronic acid, and chitosan have been most commonly used to study the biological effects of film properties on cells.[29,30,33−35] It has been shown that the electrolyte composition and assembly conditions can be varied to regulate the properties of the films, such as the thickness, surface topography, surface charge, and stiffness, all of which may alter cell adhesion, protein adsorption, and cell differentiation.[28−38] Herein, PEM films were incorporated into SLBs to produce layered microenvironmental substrates for NSPC induction and neural engineering optimization. Due to both the mobility of the fluidized polypeptide materials and the closed synaptic structure, cells can be mobilized on the basis of not only the diffusivity but also their synapse-triggering interactions.

In this study, we explored the potential of using SLBs as a platform for NSPC induction and the formation of functional neurons by adsorption with PEM films as adhesive substrates for NSPC differentiation in an in vitro culture. The following biological responses were measured for the NSPCs on the SLB−PEM and PEM substrates: neurite outgrowth length, differentiation lineage, and the synapse functionality of differentiated neurons. In vitro differentiation assays are important for characterizing cells, assaying novel instructive substrates, and generating specific cell types. The biomimetic SLB structure may provide the mobility and high structural similarity to synaptic membranes necessary to trigger synapse functionality.

2. EXPERIMENTAL SECTION

Preparation of SLB. All chemicals were purchased from commercial sources and used without further purification. Water was deionized and purified using a Milli-Q unit (Milli-Q plus, Millipore). The preparation of *N*-glutarylphosphatidylethanolamine (NGPE)-doped vesicles and the SLB formation were previously described.[21] NGPE, 10% (Avanti Polar Lipids, Alabaster, AL), mixed with 1-palmitoyl-2-oleoyl-*sn*-glycero-3-phosphocholine (POPC) (Avanti Polar Lipids) by weight was dissolved in chloroform and then dried under a gentle stream of nitrogen to form a thin lipid film on the wall of a tube. Next, the tube was placed in a vacuum for 3 h. After vesicle reconstitution in 1.0 mL of pH 5.5 Tris buffer solution with 10 mM Tris and 100 mM NaCl, the vesicle solution was extruded through a 100 nm filter (Avanti Polar Lipids), followed by extrusion through a 30 nm filter (Avanti Polar Lipids). Subsequently, the vesicle solution was transferred to hydrophilic glass for cell culture to form lipid bilayers.

Preparation of PEM Films on the SLB. An SLB with adsorbed PLL/PLGA PEM films was prepared according to a procedure described in the literature, with some modifications.[39] The physical adsorption of PEM films was performed using batch and static conditions. Initially, all polypeptides were dissolved in 10 mM Tris-HCl buffer with 0.15 M NaCl at pH 7.4. The SLB substrates were then immersed in PLL (MW 15 000−30 000; Sigma, St. Louis, MO) solution (1 mg/mL) for 10 min at room temperature, followed by rinsing with 1 mL of Tris-HCl buffer for 1 min. To couple PLGA, the SLB−PLL-coated slides were subsequently immersed in a PLGA solution (MW 3000−15 000, Sigma, St. Louis, MO, 1 mg/mL) for 10 min, followed by rinsing with 1 mL of Tris-HCl buffer for 1 min. Lastly, the substrates were cleaned with fresh PBS to remove uncoupled polypeptides. The resulting substrates were named SLB−(PLL/PLGA) (n), where n denotes the number of polyelectrolyte pairs generated by repeating the above steps; for example, an n of 0.5 refers to SLB−PLL only, and an n of 1 refers to SLB-(PLL/PLGA) (n = 1).

FRAP (Fluorescence Recovery after Photobleaching) Measurement. Before FRAP measurements, Texas Red-DHPE (TR-PE, 0.5%, w/w) (Molecular Probe, Eugene, OR) was doped into phospholipid mixtures to form liposomes the recovery of which could be traced by the FRAP images. The phospholipid vesicle solution was dropped onto cleaned, hydrophilic glass for fusion of the SLB. All fluorescence experiments were performed with confocal microscopy. The following image data were collected: a bleached image, an image immediately after bleaching, and a recovered image; the images were then analyzed using MetaMorph software (Molecular Devices, Downingtown, PA).

Isolation and Culture of Cortical NSPCs. Cerebral cortical NSPCs were isolated from ED 14−15 Wistar rat embryos using a previously described protocol with modification.[40] The animal work in this study was performed in strict accordance with the recommendations from the Institutional Animal Care and Use Committee at Chang Gung University (IUPAC permit number CGU12-084). Rat embryonic cerebral cortices were dissected, cut into small pieces, and mechanically triturated in cold Hank's balanced salt solution (HBSS). After dissociation, the cells were collected by centrifugation and resuspended in serum-free Dulbecco's modified eagle's medium (DMEM)-F12 and N2 supplement (100 mg/mL human apotransferrin, 25 mg/mL insulin, 30 nM sodium selenite, and 20 nM progesterone; pH 7.2). Quantification of live cells was performed using a trypan blue exclusion assay with a hemocytometer. NSPCs were purified and cultured in T25 culture flasks (Corning, NY) at a density of 50 000 cells/cm^2 in the medium described above, with the addition of 20 ng/mL basic fibroblast growth factor (bFGF). The cultures were maintained at 37 °C in a humidified 5% CO_2 incubator. After 1−3 days, the proliferating cells formed neurospheres, which were suspended in the medium. Then, the suspended neurospheres were collected by centrifugation, mechanically dissociated, and subcultured in a new T25 culture flask at the same density in fresh medium. The resulting cells grew into new neurospheres over the next 2−3 days, and subculturing was repeated to obtain purified NSPCs.

Immunocytochemistry. For immunocytochemical characterization, cells cultured for 5 days in vitro were fixed in ice-cold 4% paraformaldehyde in PBS for 20 min and washed three times with PBS. After fixation, the cells were incubated with the primary antibodies; the following antibodies were diluted in PBS containing 10% bovine serum albumin (BSA) and 0.3% Triton X-100 for 2 h at 37 °C: rabbit anti-microtubule associated protein 2 (MAP-2) (1:1000 dilution; Chemicon), rabbit anti-glial fibrillary acidic protein (GFAP) (1:1000 dilution; Chemicon), and synapsin I (1:1000 dilution; Chemicon). The cells were then incubated with FITC- and rhodamine-conjugated secondary antibodies for 30 min at room temperature to visualize the signal. The secondary antibodies and their dilutions were FITC-conjugated donkey anti-rabbit IgG (preabsorbed with rabbit and rat serum protein; 1:250; Chemicon), FITC-conjugated goat anti-mouse IgG (preabsorbed with rabbit and rat serum protein; 1:250; Chemicon), and rhodamine-conjugated goat anti-mouse IgG (preabsorbed with rabbit and rat serum protein;

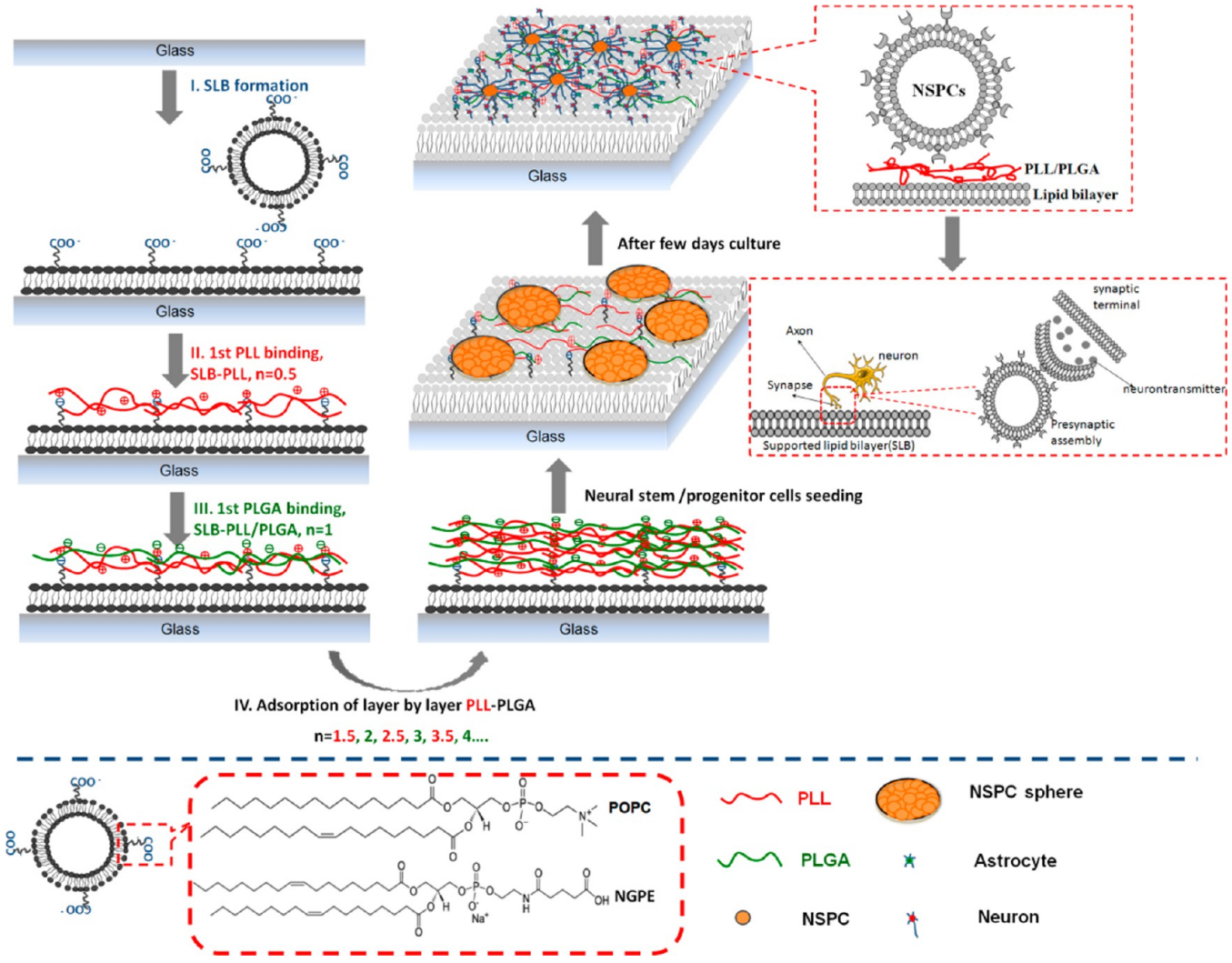

Figure 1. Schematic illustrations (not to scale) of the layer-by-layer assembly of polypeptides adsorbed onto the SLB, the NSPC seeding, and the directed NSPC differentiation. The chemical structures of POPC and NGPE are shown at the bottom. The SLB structure is similar to a synapse, and this similarity may induce the differentiation of NSPCs into functional neurons.

1:250; Chemicon). The immunostained cells were visualized using confocal microscopy. The antibodies used in this study had been previously tested and characterized in preliminary studies.

Analysis of Neurite Outgrowth. Digital photomicrographs were taken from random fields of view of cultured neurospheres at the indicated time points. The lengths of 10−15 of the longest processes on each neurosphere were measured from the edge of the neurosphere to the tip of the processes, i.e., the end-to-end distance. The process lengths were measured by tracing the processes using ImageJ. The lengths of processes from more than 15 independent neurospheres were calculated for each experiment, and the means and standard errors of the mean (SEM) were calculated.

Analysis of the Differentiation Percentage of Neural Cells. Quantitative analysis of the immunocytochemistry was performed using a microscope equipped with a standard fluorescence illuminator and a digital camera. At least three microscopic fields of view from each group were randomly taken. To calculate the percentage of differentiated cells of each phenotype, the area of glial fibrillary acid protein (GFAP) and microtubule associated protein 2 (MAP2)-positive cells was divided by the total number of cells in the neurospheres to determine the astrocyte and neuron percentages in each field, respectively. The ratios of neurons/astrocytes in each of the culture conditions were also calculated. Data were collected from three independent experiments from three different culturing sessions and analyzed using imaging software.

Labeling of Active Synapses after Culture on the Different Substrates. FM1-43 labeling of functional synapses was performed according to standard procedures described in the literature.[41] After 5 days of culture, a 90 mM KCl solution containing 2 μM of the fluorescent styryl membrane probe FM1-43 (Invitrogen) was added for 60 s, after which the cells were washed three times in normal saline for 5 min to remove surface-bound FM1-43. The normal saline consisted of 137 mM NaCl, 5.4 mM KCl, 1.3 mM $CaCl{\cdot}2H_2O$, 0.4 mM KH_2PO_4, 0.8 mM $MgSO_4$, 4 mM $NaHCO_3$, 5.6 mM D-glucose, 0.3 mM Na_2HPO_4, and 20 mM HEPES, with the pH adjusted to 7.2 using NaOH. To determine the release and turnover of synaptic vesicles, the synapses were loaded with FM1-43 and destained by 150 s stimulation with a 90 mM KCl solution in the absence of FM1-43. Fluorescence images of the FM1-43-loaded synapses were obtained using a fluorescence microscope.

Western Blot Assay. Cells were collected by gentle shaking of the wells and washed twice with PBS. The cells were lysed by treatment with ice-cold lysis buffer (20 mM Tris, pH 7.5, 150 mM NaCl, 1 mM EDTA, 1% Triton X-100, 10% glycerol, 1 mM NaF, 1 mM Na_3VO_4, and a 1:200 dilution of Protease Inhibitor Cocktail II; Calbiochem) for 30 min, followed by sonication at 4 °C for 15 s. The lysates were subsequently clarified by centrifugation at 10 000 rpm for 30 min at 4 °C, and the resulting supernatant was saved for protein analysis and Western blot analysis. The protein concentration was measured using commercial protein assay reagents (Bio-Rad, Hercules, CA). For

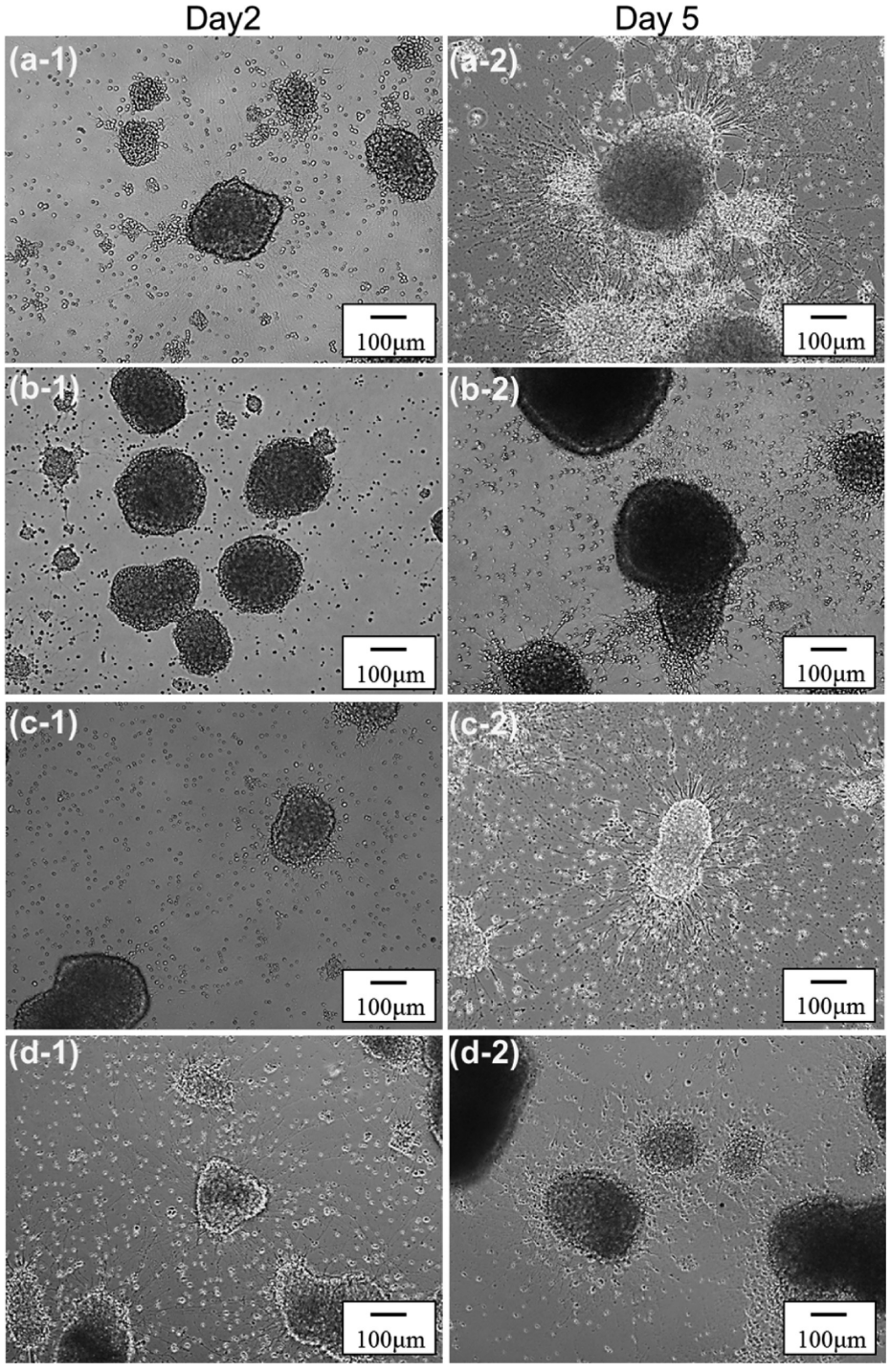

Figure 2. Phase-contrast images of the phenotypes of differentiated cells from embryonic cerebral cortical neurospheres cultured on SLB−PEM films after 2 and 5 days. (a) SLB−PEM (n = 0.5), (b) SLB−PEM (n = 1), (c) SLB−PEM (n = 7.5), and (d) SLB−PEM (n = 8).

Western blotting, the supernatant was added to an equal volume of Laemmli sample buffer (62.5 mM Tris, pH 6.8, 25% glycerol, 2% SDS, 0.01% bromophenol blue, and 5% β-mercaptoethanol) and heated to 95 °C for 5 min. Proteins (50 μg total protein per lane) were then separated by SDS−PAGE on 10% polyacrylamide gels and transferred to PVDF membranes. The membranes were blocked with 5% nonfat milk in TBST buffer (Bio-Rad, Hercules, CA). The following primary antibodies were used: rabbit MAP2 antibody (1:1000), rabbit GFAP antibody (1:2000), mouse synapsin I antibody (1:1000), and mouse GAPDH antibody (1:5000; GeneTex). The membranes were incubated with primary antibody at 4 °C overnight. After washing, the blots were incubated with HRP secondary antibodies (1:10 000; BD) at room temperature for 2−3 h. The reaction products were visualized using an enhanced chemiluminescence (ECL) Western Blot Detection Kit (Amersham Pharmacia Biotech). Densitometric quantification of the Western blots was performed using ImageJ software.

Statistical Analysis. The data are presented as the mean ± standard deviation (SD) of four to six independent experiments. The results were analyzed by Student's t test. Statistical significance is indicated as *, $^{\#}$, and $^{\&}$ for $p < 0.05$; **, $^{\#\#}$, and $^{\&\&}$ for $p < 0.01$; *** and $^{\&\&\&}$ for $p < 0.005$; and ****, $^{\#\#\#\#}$, and $^{\Delta\Delta\Delta\Delta}$ for $p < 0.001$.

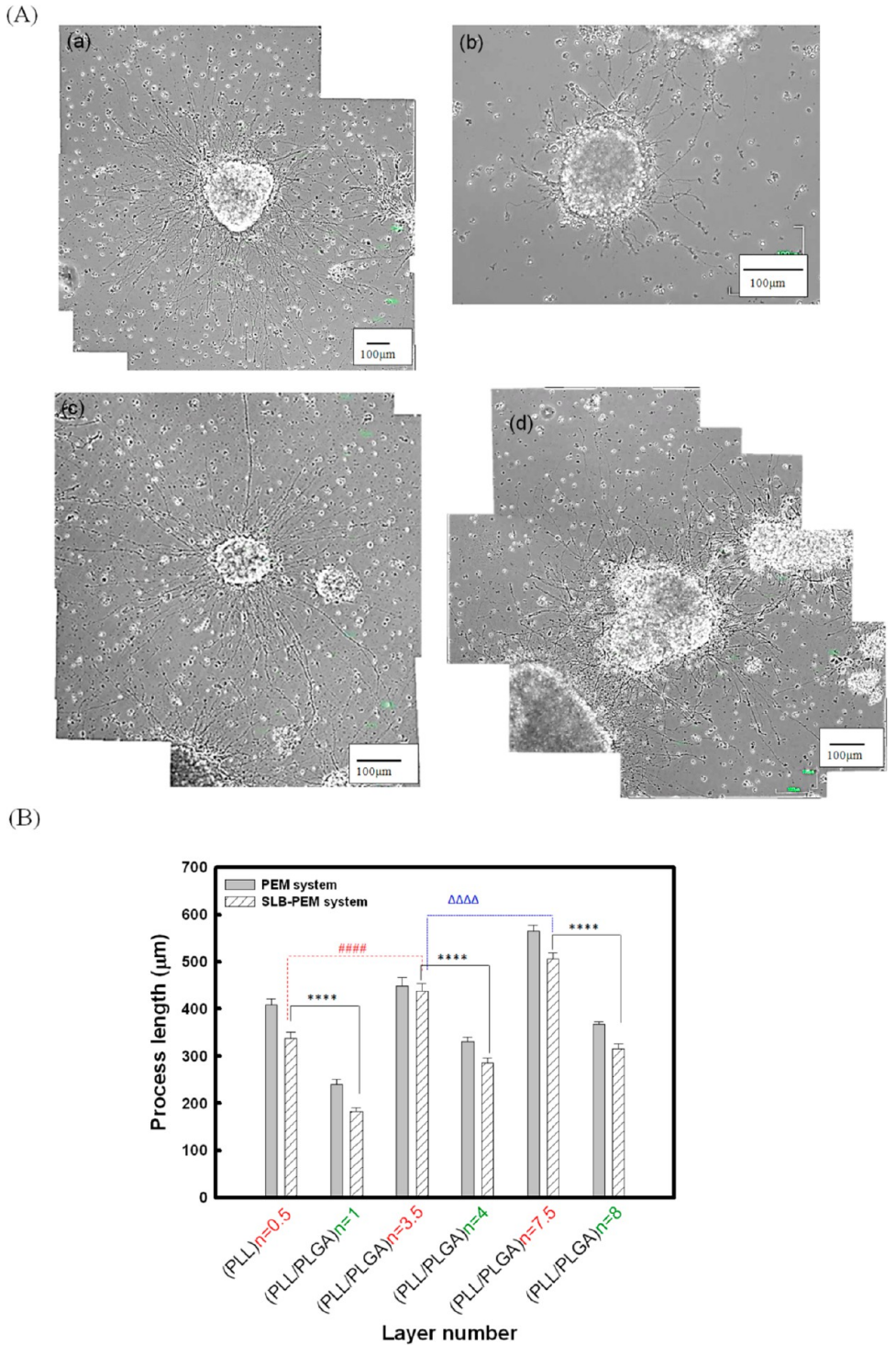

Figure 3. (A) Representative images showing the morphologies of cell processes on (a) SLB−PEM (n = 0.5), (b) SLB−PEM (n = 1), (c) SLB−PEM (n = 7.5), and (d) SLB−PEM (n = 8). (B) Quantification of the lengths of the processes extending from the neurospheres on the PEM and SLB−PEM film substrates under serum-free conditions at 250 neurospheres per cm^2 after 3 days in culture. The lengths of the 10−15 longest processes per neurosphere were estimated linearly from the edge of the neurospheres to the tip of the processes. The values represent the means ± SEM for six independent neurospheres. Asterisks denote significant differences in the average length of processes on the different PEM films ($^{****,\#\#\#\#,\Delta\Delta\Delta\Delta}p < 0.001$), as determined by Student's t test.

3. RESULTS AND DISCUSSION

SLB−PEM Film Formation, Surface Structure, And Diffusivity. The procedure of layer-by-layer PEM film adsorption on SLB−glass is illustrated in Figure 1. The formation of PEM films was achieved through electrostatic interactions between PLL as a polycation and PLGA as a polyanion. After the formation of the PEM structure, NSPCs were seeded and cultured on the layered SLB−PEM films. AFM was also used to examine the surface morphology of the SLB−PEM films on mica. A defect of the lipid bilayer on the mica surface was imaged, permitting us to measure the

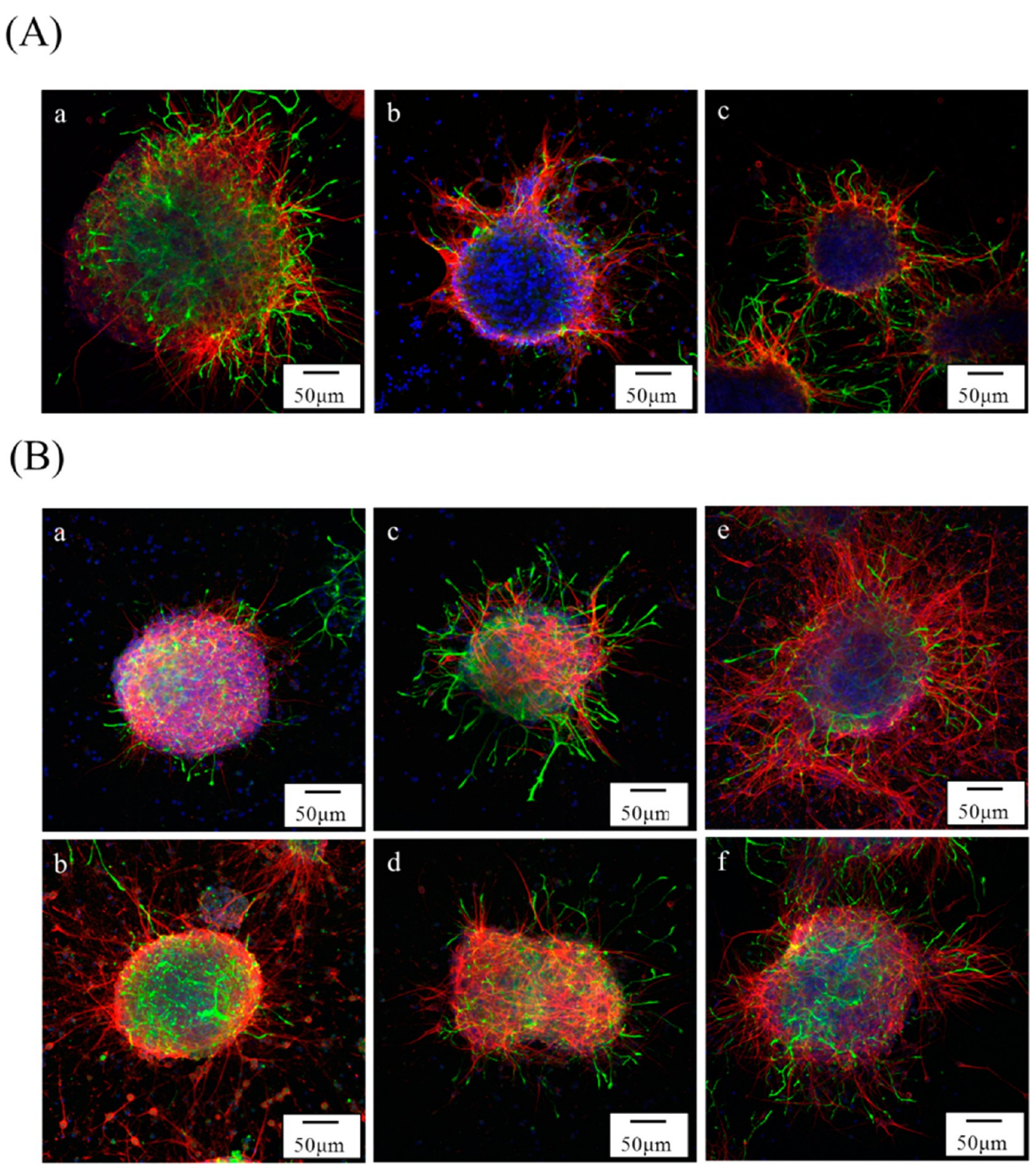

Figure 4. Fluorescence photomicrographs showing the phenotypes of the cells that differentiated from embryonic cerebral cortical neurospheres after 3 days in culture. Anti-MAP-2 (red) and anti-GFAP (green) antibodies show the immunoreaction of differentiated neurons and astrocytes, respectively. (A) Images of seeded NSPCs on PEM films. (a) PEM (n = 3.5), (b) PEM (n = 7.5), (c) PEM (n = 8). (B) Fluorescence photomicrographs of NSPCs cultured on SLB−PEM films. (a) SLB−PEM (n = 0.5), (b) SLB−PEM (n = 1), (c) SLB−PEM (n = 3.5), (d) SLB−PEM (n = 4), (e) SLB−PEM (n = 7.5), and (f) SLB−PEM (n = 8).

thickness of the lipid bilayer, which was ∼4 nm (Figure S1A, Supporting Information), consistent with the QCM-D data.

AFM was used to characterize the surface structure and roughness of the SLB−PEM films. Figure S1 (Supporting Information) shows the"heterogeneous" film topography, and the roughness increased with the number of deposited PEM film layers. In addition, the surface morphology showed some aggregation as the film thickness increased. Furthermore, because the microdomains and diffusivity of lipids are believed to play an important role in controlling cellular effects and neuronal behavior, the mobility of SLB−PEM was also confirmed here. Lateral lipid diffusivity in the SLB−PEM films was evaluated by fluorescence recovery after photobleaching (FRAP). For the SLBs without PEM, the recovery

was fast and relatively complete (Figure S2A, Supporting Information), and the diffusion coefficient was approximately 1.135. The relative diffusion coefficient decreased slightly to 0.709 as the number of film layers increased to $n = 5$. These results indicate that the SLB−PEM films could maintain some of the mobility.

Morphological Characteristics of NSPCs on SLB−PEM Films. NSPCs were seeded on layered SLB−PEM films at an initial density of 250 neurospheres per well in serum-free medium. Figure 2 shows photomicrographs of differentiated cell phenotypes from embryonic cerebral cortical neurospheres cultured on SLB−PEM films after 2 and 5 days of incubation. Glass-only and glass−SLB substrates were not suitable for NSPC attachment and differentiation (not shown here). In contrast, glass modified with an SLB−PEM surface promoted cell attachment and differentiation for all of the SLB−PEM films, even in a serum-free and reagent-free medium, and cells were observed to migrate out of the neurospheres. As shown in Figure 2, the cells differentiated into neural-related cells and formed neural networks after 5 days of culture. This phenomenon is consistent with and similar to what has been observed for NSPCs cultured on PLL/PLGA PEM films. Attached neurospheres with processes extending out from the spheres were observed, especially on the SLB−PEM films having a PLL terminal layer. Ren et al. also reported that the communication and migration of NSPCs were influenced by surface chemistry.[42] In addition, the cells displayed longer processes on SLB−PEM ($n = 7.5$) than on SLB−PLL ($n = 0.5$) or SLB−PEM ($n = 1$), as indicated when comparing parts c-2 and a-2 of Figure 2. The phase-contrast images of these cells revealed a morphology that indicates many presumptive neurons and extended processes. In summary, these results show that cells displayed longer processes and better neural networks as the number of layers increased, especially when the final layer had a positive charge.

Measurement of NSPC Neurite Outgrowth on SLB−PEM Films. Figure 3 shows photomicrographs and quantitative measurements of the neurite outgrowth from NSPCs on PEM and SLB−PEM films. Images of one sphere were constructed from several photographs. As shown in Figure 3A(b),A(d), the cells displayed short and crooked processes on the SLB−PEM films that had PLGA as the terminal layer. In contrast, many long and straight processes were observed when the neurospheres were cultured on the SLB−PEM films that had PLL as the terminal layer [Figure 3A(a),A(c)]. Thus, the surface charge of the outmost layers affected the process length and morphology. In addition, measurements of the process lengths for 10 spheroids on layered PEM and SLB−PEM films are compared in Figure 3B. In general, the average process lengths on the PEM film substrates were slightly longer than those on the SLB−PEM film substrates. Synthetic SLBs provide a nonfouling surface that resists protein adsorption and prevents nonspecific molecular and cellular interactions. Although the fluidity of the SLB closely mimics that of a live cell surface, the fluidity may reduce the stability of cell−substrate contacts. Cell adhesion is one of the factors that affects neurite outgrowth; thus, it is assumed herein that the nonfouling property and fluidity of SLBs may decrease the process length compared with that for the PEM-only system. Furthermore, the processes had a length of 200−400 μm after 3 days of culture when PLGA was the terminal layer; in contrast, the length was 400−600 μm after 3 days of culture when PLL was the terminal layer. As shown in Figure 3B, the process length of NSPCs cultured on SLB−PEM films with PLL as the terminal layer was significantly different from that of the corresponding groups cultured on SLB−PEM films with a PLGA terminal layer ($^{****}p < 0.001$). In addition, the process length on the SLB−PEM films that had a high number of layers was significantly different compared with that on substrates having fewer layers [PEM ($n = 3.5$), $^{\#\#\#\#}p < 0.001$; PEM ($n = 7.5$), $^{\Delta\Delta\Delta\Delta}p < 0.001$). The average length was increased to as high as 500 μm on SLB−PEM ($n = 7.5$) after 3 days of culture, without the addition of growth factors or serum. Wang et al. has used the synthesis of a lysine-alanine sequential (LAS) polymer substrate to induce NSPCs, and they found that the process length of NSPCs on the LAS substrate increased up to 400 μm after 4 days of culture.[40] In addition, Zhang et al. also tried to use a conducting polymer, polypyrrole doped with laminin peptides, to induce the differentiation of adult NSPCs, and the process length of NSPCs was increased to 250 μm after 14 days of culture.[7] Our result revealed that the average length was increased to as high as 500 μm on SLB−PEM ($n = 7.5$) after only 3 days of culture, which indicates that the layer-by-layer assembled PEM and SLB−PEM films are ideal for NSPC attachment and differentiation and can stimulate process outgrowth. Furthermore, the enhanced process outgrowth may be due to variations in the surface niche. The overall extent of process growth by the NSPCs on PEM films and SLB−PEM films was satisfactory. The results demonstrate that process outgrowth from adhered NSPCs is dependent on both the chemistry of the terminal layer and the number of layers.

Differentiation of NSPCs on SLB−PEM Films. NSPCs have the ability to differentiate into specific neural-related cells. However, their differentiation fate cannot be evaluated using only their morphologies. Immunostaining with specific antibodies has been widely used to analyze specific cell phenotypes. Herein, the expression of the neuron marker MAP-2 (red) and the astrocyte marker GFAP (green) was used to determine the type of the differentiated cells.

The immunostaining results for GFAP and MAP2 on PEM ($n = 3.5$), PEM ($n = 7.5$), and PEM ($n = 8$) are shown in Figure 4A. In addition, Figure 4B shows the expression level of GFAP and MAP2 on SLB−PEM film substrates ranging from 0.5 to 8 layers. These results show more MAP-2-positive neuronal cells migrated away from the neurospheres on the SLB−PEM films with a PLL terminal layer. Furthermore, the quantity increased as the number of layers increased, as indicated when comparing parts B(a) and B(e) of Figure 4. Obviously, the expression of MAP-2 on the SLB−PEM films was much higher than that on the PEM films without a SLB base, as indicated by comparisons of parts A(b) and B(e) of Figure 4. MAP-2 especially showed very high expression on SLB−PEM ($n = 7.5$), indicating that the substrate niche strongly regulated the differentiation tendencies.

To quantify the number of differentiated cells of each phenotype on the layered PEM and SLB−PEM films, the number of MAP-2- and GFAP-positive cells in 10 neurospheres was counted. Figure 5 shows the results from the quantification of the differentiation percentage after 5 days of culture. As shown in Figure 5A,C, the percentage of neurons on both systems with a PLL terminal layer was higher than that with a PLGA terminal layer. It is believed that a positive charge is required for substrate−axon adhesive interactions, which may also enhance neuron induction. In addition, the quantity of differentiated neurons also increased significantly as the layer number increased [$^{**}p < 0.01$ for SLB−PEM ($n = 3.5$), $^{****}p$

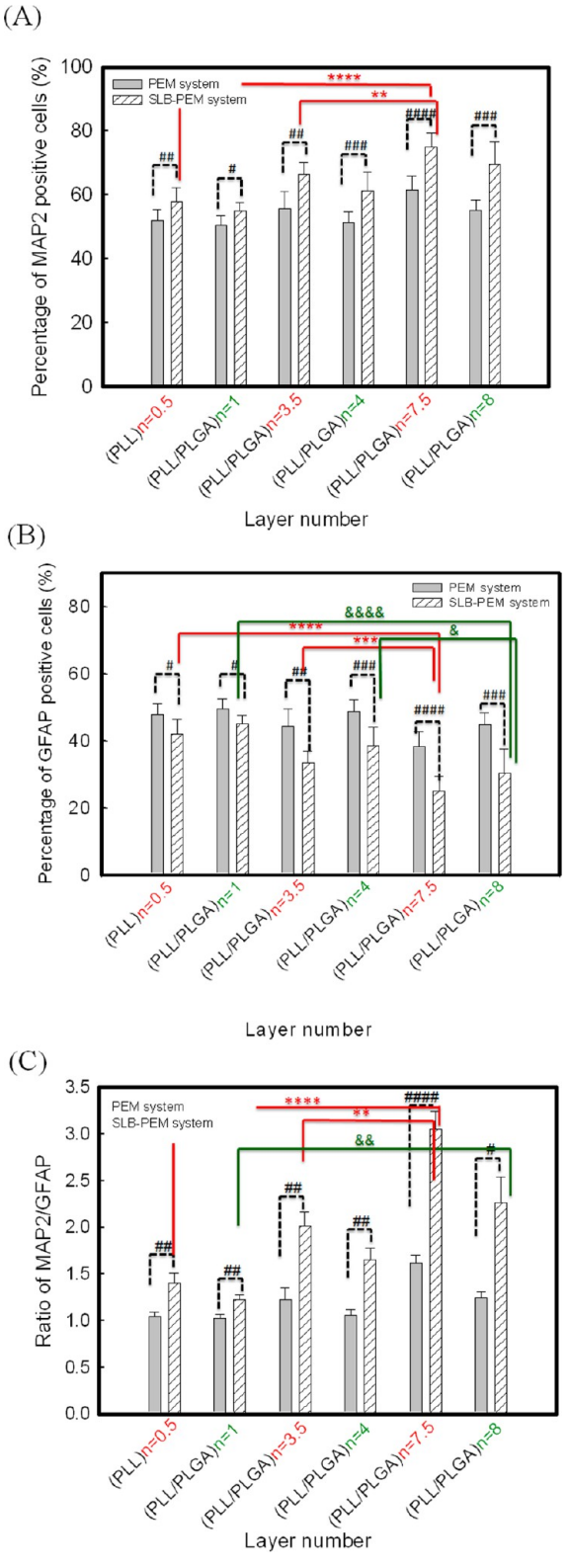

Figure 5. Quantification of the percentage of differentiation into (A) neurons and (B) astrocytes and (C) the ratio of neurons/astrocytes for neurospheres on the PEM and SLB−PEM substrates. The cells were cultured under serum-free conditions at 250 neurospheres per cm^2 for 5 days. # denotes significant differences in the neuron percentage between the PEM and SLB−PEM systems ($^{\#,\&}p < 0.05$; $^{**,\#\#,\&\&}p < 0.01$; $^{\#\#\#,\&\&\&}p < 0.005$; $^{\#\#\#\#,****}p < 0.001$), as determined by Student's *t* test.

< 0.001 for SLB−PEM (n = 7.5), and $^{\&\&}p < 0.01$ for SLB−PEM (n = 8)]. Most importantly, comparing the SLB−PEM system and the PEM-only system indicates that the expression of MAP-2 and the ratio of MAP2/GFAP were significantly different ($^{\#}p < 0.05$, $^{\#\#}p < 0.01$, $^{\#\#\#}p < 0.005$, and $^{\#\#\#\#}p < 0.001$). In a previous study, PLL-coated latex beads and PDL were used to form presynaptic-like endings and functional synapses with hippocampal neurons.[25,43] Because this study provides a very simple and pure culture condition, without requiring the addition of serum or growth factors, these results suggests that SLB-based substrates may affect the differentiation tendency and trigger NSPCs to differentiate into neurons.

Functionality of Differentiated Neurons: Immunostaining of Synapsin I and Analysis of Functionally Active Synapses. One of the key functionalities of mature CNS neurons is their ability to form synapses. To determine whether the differentiated neurons from NSPCs on the SLB−PEM films displayed synapse function, immunostaining of synapsin I and an analysis of functionally active synapses were performed. Punctate staining of synapsin I revealed that the synaptic vesicle protein was concentrated at synapses in the neurons differentiated from the NSPCs on SLB−PEM films (Figure 6A). Furthermore, the staining was more obvious on the substrates with a positively charged terminal layer. Coexpression of synapsin I and MAP-2, indicated by double staining, is also shown in Figure 6B. Because synapsin I is a marker of presynaptic terminals, which occur in axons, and MAP-2 is a marker for dendrites, the expression of synapsin I was observed as long tracks that were far from the cell body. In contrast, the expression of MAP-2 displayed a more branched appearance and was near the cell body. The patterns of differentiated cells on the SLB−PEM films were also observed. The results showed that the neurons formed dense networks with a large number of neurites and neural filaments.

Moreover, Figure 6C shows the functionality test for active synapses on SLB−PEM (n = 7.5) and the results quantifying the relative fluorescence intensities. The membranes of synaptic vesicles were stained with the FM1-43 lipid dye. After stimulation by a high potassium solution, the fluorescence intensity of the lipid dye decreased after the second stimulation by the high potassium solution without lipid dye. This result indicated that the synaptic vesicles were functional and recyclable, and it supports our hypothesis that SLB-based PEM films can stimulate the differentiation of NSPCs into neurons and trigger synaptic function by providing adhesive contacts.

Quantification of Protein Expression of NSPCs on SLB−PEM Films by Western Blot. To quantitatively evaluate the protein expression of NSPCs on layered SLB−PEM films after 5 days of culture, Western blot analysis was used to determine the expression levels of MAP2, GFAP, and synapsin I. Figure 7 shows that the MAP2 expression was higher on SLB−PEM (n = 7.5) than on SLB−PEM (n = 0.5) and that the expression on SLB−PEM (n = 8) was higher than that on SLB−PEM (n = 1). The SLB−PEM films with PLL terminal layers displayed higher expression of MAP2 compared with the films with PLGA terminal layers. These results were consistent with the quantification of the fluorescence intensity, which is shown in Figure 5A. Moreover, the protein concentration and fluorescence intensity results for GFAP expression (Figure 7B) and the relative ratio of MAP2/GFAP (Figure 7C) also correlated well (Figures 5 and 7). Furthermore, the neuron functionality of NSPCs cultured on SLB−PEM (n = 0.5) and

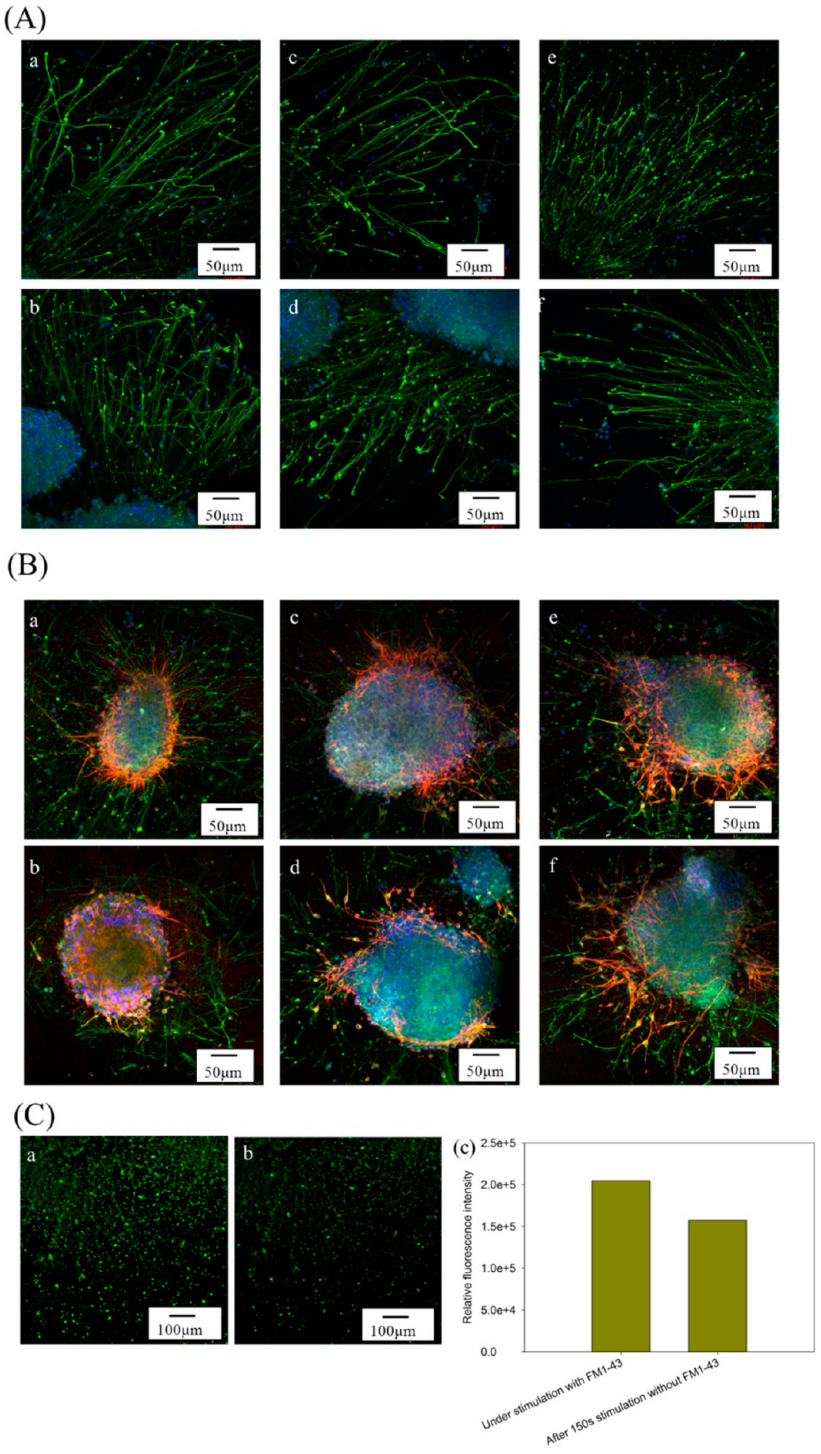

Figure 6. Fluorescence photomicrographs showing the phenotypes of the differentiated cells obtained from embryonic cerebral cortical neurospheres after 3 days of culture. (A) The images of NSPCs cultured on SLB−PEM films show the immunoreactivity for synapsin I, indicating functional neurons. (a) SLB−PEM (n = 0.5), (b) SLB−PEM (n = 1), (c) SLB−PEM (n = 3.5), (d) SLB−PEM (n = 4), (e) SLB−PEM (n = 7.5), and (f) SLB−PEM (n = 8). (B) Immunostaining for MAP2 and synapsin I. (a) SLB−PEM (n = 0.5), (b) SLB−PEM (n = 1), (c) SLB−PEM (n = 3.5), (d) SLB−PEM (n = 4), (e) SLB−PEM (n = 7.5), and (f) SLB−PEM (n = 8). (C) FM1−43 labeling showing the recycling of synaptic vesicles on SLB−PEM (n = 7.5) before (a) and 100 s after (b) the start of stimulation with a high concentration of KCl. Scale bars = 100 μm. (c) Quantification of the relative fluorescence intensity before and after stimulation.

PEM (n = 7.5) was measured by quantifying the level of synapsin I protein expression. As shown in Figure 7D, the cells displayed a higher expression level of synapsin on SLB−PEM (n = 7.5) and SLB−PEM (n = 8) than on SLB−PEM (n = 0.5) and SLB−PEM (n = 1), respectively. In addition, as shown in Figure 7E, the cells displayed a high expression level of synapsin I on SLB−PEM (n = 7.5) and SLB−PEM (n = 0.5), and these levels were significantly different from those on PEM (n = 7.5) and PEM (n = 0.5), respectively. Thus, the SLB-based substrate not only enhances neuron differentiation but also induces

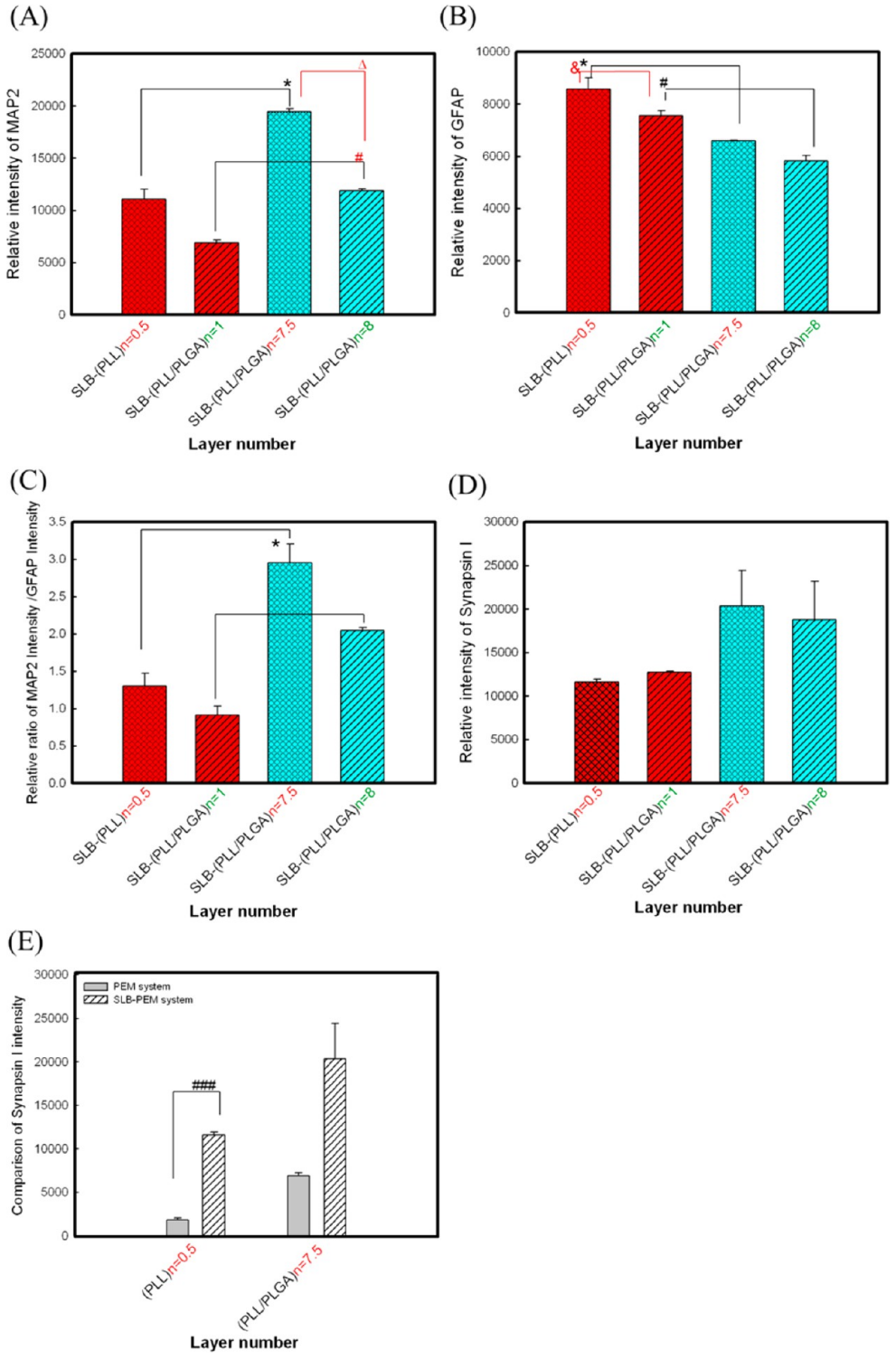

Figure 7. Western blots were performed with anti-MAP2, anti-GFAP, anti-synapsin I, and anti-actin antibodies for NSPCs cultured on SLB−PEM films for 5 days. (A) Relative intensity of MAP2 expression on the SLB−PEM films. (B) Relative intensity of GFAP expression on the SLB−PEM films. (C) Relative ratio of MAP2/GFAP intensity. (D) Relative intensity of synapsin I expression on the SLB−PEM films. (E) Relative intensity of synapsin I expression on the PEM and SLB−PEM substrates. The intensities were determined by band densitometry analysis. Asterisks denote significant differences in neuron percentage between the different PEM film conditions ($*^{,\#}p < 0.05$), as determined by Student's t test.

synaptic function. Furthermore, as shown in Figure 5C, the neuron percentage on SLB−PEM (n = 7.5) and SLB−PEM (n = 8) was higher than that on SLB−PEM (n = 0.5) and SLB−PEM (n = 1), which is consistent with the result of the synapsin expression level. This result further confirmed that SLB−PEM (n = 7.5) films could induce the differentiation of NSPCs into functional neurons and encourage strong axonal growth and synaptogenesis.

These findings suggest that there are three factors affecting the differentiation tendency of NSPCs in this system: the terminal layer, the number of layers, and the presence of an SLB base. Collectively, these results suggested that the SLB

base may trigger the differentiation of the neurons and that the PEM films may consolidate the film structure and enhance the cell migration. In addition, the SLB−PEM films with PLL terminal layers provide a positive charge to enhance cell adhesion, and the primary amine moieties may contribute to a chemoselective process. Furthermore, previous studies have verified that the stiffness of PEM films decreases as the number of layers increases, and many researchers have reported that softer materials greatly favor neurons, while stiffer surfaces promote glial cultures, which may explain the high enhanced neuron differentiation ratio on SLB−PEM (n = 7.5).[2,4]

4. CONCLUSIONS

In conclusion, a neuron induction system was fabricated in this study by the layer-by-layer assembly of PLL/PLGA PEM films and an SLB base to regulate the adhesion of NSPCs and the differentiation of NSPCs into functional neurons. PEM films were used to produce a layered microenvironment of surfaces that promote cell adhesion and differentiation; the neurite outgrowth, the types of differentiated cells, and the synaptic function were all regulated by the PEM layer number and the composition of the outmost layer. The SLB base may trigger neuron differentiation, as this approach resulted in enhanced differentiation of NSPCs into neurons on SLB−PEM films. This study provides a biomimetic system that stimulates NSPC differentiation and is drastically different from other synthetic materials, and the results indicate that key targets of neural engineering were achieved, including long processes, a large neural network size, and a large number of functional neurons. These findings may provide a useful tool, as well as new strategies for surface modification, to create and optimize stem cell niches for neural engineering.

■ ASSOCIATED CONTENT

Ⓢ Supporting Information

Figure S1 shows TM-AFM height images of adsorbed PEM films on SLB, and Figure S2 shows quantitative traces of the normalized fluorescence intensity across the bleached spot after 30 min. This material is available free of charge via the Internet at http://pubs.acs.org/.

■ AUTHOR INFORMATION

Corresponding Author

*Phone: +886 2 2118800, ext 5985. E-mail: iclee@mail.chu.edu.tw.

Notes

The authors declare no competing financial interest.

■ ACKNOWLEDGMENTS

We thank Chang Gung University for providing financial support. We also received a Summit Project grant from the National Science Council (grant NSC 101-2221-E-182-012 to I.-C.L.). We also thank Dr. Ying-Chih Chang for instrument support.

■ REFERENCES

(1) Beduer, A.; Vieu, C.; Arnauduc, F.; Sol, J. C.; Loubinoux, I.; Vaysse, L. Engineering of Adult Human Neural Stem Cells Differentiation through Surface Micropatterning. *Biomaterials* **2012**, *33*, 504−514.

(2) Camci-Unal, G.; Cuttica, D.; Annabi, N.; Demarchi, D.; Khademhosseini, A. Synthesis and Characterization of Hybrid Hyaluronic Acid−Gelatin Hydrogels. *Biomacromolecules* **2013**, *14*, 1085−1092.

(3) Johnson, P. J.; Wood, M. D.; Moore, A. M.; Mackinnon, S. E. Tissue Engineered Constructs for Peripheral Nerve Surgery. *European Surgery: ACA: Acta Chirurgica Austriaca* **2013**, *45*, 122−135.

(4) Li, X.; Liu, X.; Zhang, N.; Wen, X. Engineering in Situ Crosslinkable, Injectable, and Neurocompatible Hydrogels. *J. Neurotrauma* **2014**, DOI: 10.1089/neu.2013.3215.

(5) Matyash, M.; Despang, F.; Mandal, R.; Fiore, D.; Gelinsky, M.; Ikonomidou, C. Novel Soft Alginate Hydrogel Strongly Supports Neurite Growth and Protects Neurons against Oxidative Stress. *Tissue Eng. Part A* **2012**, *18*, 55−66.

(6) Xie, H.; Li, J.; Li, L.; Dong, Y.; Chen, G. Q.; Chen, K. C. Enhanced Proliferation and Differentiation of Neural Stem Cells Grown on PHA Films Coated with Recombinant Fusion Proteins. *Acta Biomater.* **2013**, *9*, 7845−7854.

(7) Zhang, L.; Stauffer, W. R.; Jane, E. P.; Sammak, P. J.; Cui, X. T. Enhanced Differentiation of Embryonic and Neural Stem Cells to Neuronal Fates on Laminin Peptides Doped Polypyrrole. *Macromol. Biosci.* **2010**, *10*, 1456−1464.

(8) Kim, Y. S.; Park, C. H. Dopamine Neuron Generation from Human Embryonic Stem Cells. *Int. J. Stem Cells* **2011**, *4*, 85−87.

(9) Ko, J. Y.; Lee, J. Y.; Park, C. H.; Lee, S. H. Effect of Cell-Density on in-Vitro Dopaminergic Differentiation of Mesencephalic Precursor Cells. *Neuroreport* **2005**, *16*, 499−503.

(10) Li, Y. C.; Lin, Y. C.; Young, T. H. Combination of Media, Biomaterials and Extracellular Matrix Proteins To Enhance the Differentiation of Neural Stem/Precursor Cells into Neurons. *Acta Biomater.* **2012**, *8*, 3035−3048.

(11) Li, Y.; Weiss, M.; Yao, L. Directed Migration of Embryonic Stem Cell-Derived Neural Cells in an Applied Electric Field. *Stem Cell Rev.* **2014**, DOI: 10.1007/s12015-014-9518-z.

(12) Yuan, T.; Liao, W.; Feng, N. H.; Lou, Y. L.; Niu, X.; Zhang, A. J.; Wang, Y.; Deng, Z. F. Human Induced Pluripotent Stem Cell-Derived Neural Stem Cells Survive, Migrate, Differentiate, and Improve Neurological Function in a Rat Model of Middle Cerebral Artery Occlusion. *Stem Cell Res. Ther.* **2013**, *4*, 73−82.

(13) Lim, S. H.; Liu, X. Y.; Song, H.; Yarema, K. J.; Mao, H. Q. The Effect of Nanofiber-Guided Cell Alignment on the Preferential Differentiation of Neural Stem Cells. *Biomaterials* **2010**, *31*, 9031−9039.

(14) Francis, K. R.; Wei, L. Human Embryonic Stem Cell Neural Differentiation and Enhanced Cell Survival Promoted by Hypoxic Preconditioning. *Cell Death Dis.* **2010**, *1*, e22.

(15) Kim, M.; Habiba, A.; Doherty, J. M.; Mills, J. C.; Mercer, R. W.; Huettner, J. E. Regulation of Mouse Embryonic Stem Cell Neural Differentiation by Retinoic Acid. *Dev. Biol.* **2009**, *328*, 456−471.

(16) Tan, J. C.; Li, Y.; Qu, W. Y.; Liu, L. Y.; Jiang, L.; Sun, K. L. Derivation of Embryonic Stem Cell Line from Frozen Human Embryos and Neural Differentiation. *Neuroreport* **2008**, *19*, 1451−1455.

(17) Daadi, M. M. In Vitro Assays for Neural Stem Cell Differentiation: Induction of Dopaminergic Phenotype. *Methods Mol. Biol.* **2008**, *438*, 205−212.

(18) Kam, L.; Boxer, S. G. Cell Adhesion to Protein-Micropatterned-Supported Lipid Bilayer Membranes. *J. Biomed. Mater. Res.* **2001**, *55*, 487−495.

(19) Wu, J. C.; Tseng, P. Y.; Tsai, W. S.; Liao, M. Y.; Lu, S. H.; Frank, C. W.; Chen, J. S.; Wu, H. C.; Chang, Y. C. Antibody Conjugated Supported Lipid Bilayer for Capturing and Purification of Viable Tumor Cells in Blood for Subsequent Cell Culture. *Biomaterials* **2013**, *34*, 5191−5199.

(20) Hain, N.; Gallego, M.; Reviakine, I. Unraveling Supported Lipid Bilayer Formation Kinetics: Osmotic Effects. *Langmuir* **2013**, *29*, 2282−2288.

(21) Huang, C. J.; Cho, N. J.; Hsu, C. J.; Tseng, P. Y.; Frank, C. W.; Chang, Y. C.; Type, I. Collagen-Functionalized Supported Lipid Bilayer as a Cell Culture Platform. *Biomacromolecules* **2010**, *11*, 1231−1240.

(22) Jonsson, M. P.; Jonsson, P.; Dahlin, A. B.; Hook, F. Supported Lipid Bilayer Formation and Lipid-Membrane-Mediated Biorecognition Reactions Studied With a New Nanoplasmonic Sensor Template. *Nano Lett.* **2007**, *7*, 3462−3468.
(23) Gedeon, P. C.; Indarte, M.; Surratt, C. K.; Madura, J. D. Molecular Dynamics of Leucine and Dopamine Transporter Proteins in a Model Cell Membrane Lipid Bilayer. *Proteins* **2010**, *78*, 797−811.
(24) Sato, M.; Inoue, K.; Kasai, M. Ion Channels on Synaptic Vesicle Membranes Studied by Planar Lipid Bilayer Method. *Biophys. J.* **1992**, *63* (6), 1500−1505.
(25) Lucido, A. L.; Suarez Sanchez, F.; Thostrup, P.; Kwiatkowski, A. V.; Leal-Ortiz, S.; Gopalakrishnan, G.; Liazoghli, D.; Belkaid, W.; Lennox, R. B.; Grutter, P.; Garner, C. C.; Colman, D. R. Rapid Assembly of Functional Presynaptic Boutons Triggered by Adhesive Contacts. *J. Neurosci.* **2009**, *29*, 12449−12466.
(26) Pautot, S.; Lee, H.; Isacoff, E. Y.; Groves, J. T. Neuronal Synapse Interaction Reconstituted between Live Cells and Supported Lipid Bilayers. *Nat. Chem. Biol.* **2005**, *1*, 283−289.
(27) Jones, E. V.; Cook, D.; Murai, K. K. A Neuron−Astrocyte Co-Culture System To Investigate Astrocyte-Secreted Factors in Mouse Neuronal Development. *Methods Mol. Biol.* **2012**, *814*, 341−352.
(28) Davila, J.; Chassepot, A.; Longo, J.; Boulmedais, F.; Reisch, A.; Frisch, B.; Meyer, F.; Voegel, J. C.; Mesini, P. J.; Senger, B.; Metz-Boutigue, M. H.; Hemmerle, J.; Lavalle, P.; Schaaf, P.; Jierry, L. Cyto-Mechanoresponsive Polyelectrolyte Multilayer Films. *J. Am. Chem. Soc.* **2012**, *134*, 83−86.
(29) Yamanlar, S.; Sant, S.; Boudou, T.; Picart, C.; Khademhosseini, A. Surface Functionalization of Hyaluronic Acid Hydrogels by Polyelectrolyte Multilayer Films. *Biomaterials* **2011**, *32*, 5590−5599.
(30) Wilson, J. T.; Cui, W.; Kozlovskaya, V.; Kharlampieva, E.; Pan, D.; Qu, Z.; Krishnamurthy, V. R.; Mets, J.; Kumar, V.; Wen, J.; Song, Y.; Tsukruk, V. V.; Chaikof, E. L. Cell Surface Engineering with Polyelectrolyte Multilayer Thin Films. *J. Am. Chem. Soc.* **2011**, *133*, 7054−7064.
(31) Chien, H. W.; Wu, S. P.; Kuo, W. H.; Wang, M. J.; Lee, C.; Lai, J. Y.; Tsai, W. B. Modulation of Hemocompatibility of Polysulfone by Polyelectrolyte Multilayer Films. *Colloids Surf., B* **2010**, *77*, 270−278.
(32) Tsai, W. B.; Chen, Y. H.; Chien, H. W. Collaborative Cell-Resistant Properties of Polyelectrolyte Multilayer Films and Surface PEGylation on Reducing Cell Adhesion to Cytophilic Surfaces. *J. Biomater. Sci. Polym. Ed.* **2009**, *20*, 1611−1628.
(33) Picart, C. Polyelectrolyte Multilayer Films: From Physico-Chemical Properties to the Control of Cellular Processes. *Curr. Med. Chem.* **2008**, *15*, 685−697.
(34) Tsai, H. A.; Wu, R. R.; Lee, I. C.; Chang, H. Y.; Shen, C. N.; Chang, Y. C. Selection, Enrichment, And Maintenance of Self-Renewal Liver Stem/Progenitor Cells Utilizing Polypeptide Polyelectrolyte Multilayer Films. *Biomacromolecules* **2010**, *11*, 994−1001.
(35) Boudou, T.; Crouzier, T.; Ren, K.; Blin, G.; Picart, C. Multiple Functionalities of Polyelectrolyte Multilayer Films: New Biomedical Applications. *Adv. Mater.* **2010**, *22*, 441−467.
(36) Gribova, V.; Gauthier-Rouviere, C.; Albiges-Rizo, C.; Auzely-Velty, R.; Picart, C. Effect of RGD Functionalization and Stiffness Modulation of Polyelectrolyte Multilayer Films on Muscle Cell Differentiation. *Acta Biomater.* **2013**, *9*, 6468−6480.
(37) Thebaud, N. B.; Bareille, R.; Daculsi, R.; Bourget, C.; Remy, M.; Kerdjoudj, H.; Menu, P.; Bordenave, L. Polyelectrolyte Multilayer Films Allow Seeded Human Progenitor-Derived Endothelial Cells To Remain Functional under Shear Stress In Vitro. *Acta Biomater.* **2010**, *6*, 1437−1445.
(38) Moby, V.; Kadi, A.; de Isla, N.; Stoltz, J. F.; Menu, P. Polyelectrolyte Multilayer Films: Effect of the Initial Anchoring Layer on the Cell Growth. *Bio-Med. Mater. Eng.* **2008**, *18*, 199−204.
(39) Richert, L.; Lavalle, P.; Vautier, D.; Senger, B.; Stoltz, J. F.; Schaaf, P.; Voegel, J. C.; Picart, C. Cell Interactions with Polyelectrolyte Multilayer Films. *Biomacromolecules* **2002**, *3*, 1170−1178.
(40) Wang, J. H.; Hung, C. H.; Young, T. H. Proliferation and Differentiation of Neural Stem Cells on Lysine-Alanine Sequential Polymer Substrates. *Biomaterials* **2006**, *27*, 3441−3450.
(41) Ma, W.; Fitzgerald, W.; Liu, Q. Y.; O'Shaughnessy, T. J.; Maric, D.; Lin, H. J.; Alkon, D. L.; Barker, J. L. CNS Stem and Progenitor Cell Differentiation Into Functional Neuronal Circuits in Three-Dimensional Collagen Gels. *Exp. Neurol.* **2004**, *190*, 276−288.
(42) Ren, Y. J.; Zhang, H.; Huang, H.; Wang, X. M.; Zhou, Z. Y.; Cui, F. Z.; An, Y. H. In Vitro Behavior of Neural Stem Cells In Response to Different Chemical Functional Groups. *Biomaterials* **2009**, *30*, 1036−1044.
(43) Burry, R. W. Formation of Apparent Presynaptic Elements In Response to Poly-Basic Compounds. *Brain Res.* **1980**, *184*, 85−98.